J. Fluid Mech. (1993), *vol.* 248, *pp.* 203–217

On equatorially trapped boundary inertial waves

By K. ZHANG

Department of Mathematics, University of Exeter, Exeter, EX4 4QJ, UK

(Received 20 February 1992 and in revised form 10 September 1992)

Solutions of the Poincaré equation describing equatorially trapped three-dimensional boundary travelling waves in rotating spherical systems are discussed. It is shown that the combined effects of Coriolis forces and spherical curvature enable the equatorial region to form an equatorial waveguide tube with characteristic latitudinal radius $(2/m)^{\frac{1}{2}}$ and radial radius $(1/m)$, where m is azimuthal wavenumber. Inertial waves with sufficiently simple structure along the axis of rotation and sufficiently small azimuthal wavelength must be trapped in the equatorial waveguide tube. The structure and frequency of the inertial waves are thus hardly affected by the presence of an inner sphere or by the condition of higher latitudes. Further calculations on rotating spherical fluid shells of finite internal viscosity and stress-free boundaries are also discussed.

1. Introduction

The equatorial zone is a particularly intriguing and interesting region in the study of wave motions in rotating spherical systems. It is a region where the Coriolis parameter decreases rapidly and the widely used quasi-geostrophic approximation breaks down. The influence of Coriolis forces on fluid motions in rotating systems, however, is usually closely associated with the curvature of a fluid container (Busse 1982). In this connection, the influence of the Coriolis forces is strongest in the equatorial region because the spherical curvature with respect to the axis of rotation is largest there. This paper is concerned with the azimuthally travelling inertial wave that is trapped in an equatorial waveguide tube with characteristic latitudinal radius $L_1 = (2/m)^{\frac{1}{2}}$ and radial radius $L_r = (1/m)$, a consequence of the combined effects of the Coriolis forces and equatorial curvature, where m is the azimuthal wavenumber of the inertial wave.

The basic equation governing wave motions in rotating fluid systems was derived by Poincaré in 1892 (see Greenspan 1969). Consider a homogeneous fluid sphere of viscosity ν that is rotating uniformly with a constant angular velocity Ω. Using the radius of the sphere, r_o, as a characteristic length, and Ω^{-1} as a characteristic scale of time, the dimensionless equation of motion and the law of conservation of mass are

$$\frac{\partial \boldsymbol{u}}{\partial t} + 2\boldsymbol{k} \times \boldsymbol{u} = -\nabla P, \tag{1}$$

$$\nabla \cdot \boldsymbol{u} = 0, \tag{2}$$

where $\boldsymbol{k}$ is a unit vector parallel to the axis of rotation, and $\boldsymbol{u}$ represents the velocity field, (u_s, u_ϕ, u_z) in cylindrical coordinates (s, ϕ, z) and (u_r, u_θ, u_ϕ) the velocity in spherical coordinates (r, θ, ϕ); P is a reduced pressure field. The Ekman number E and the Rossby number Ro, defined as

$$E = \nu/\Omega r_o^2, \quad Ro = U/\Omega r_o,$$

where U is the typical amplitude of the velocity, are set to zero. By eliminating $\boldsymbol{u}$ from (1) and (2), we obtain an equation governing inertial oscillations of an inviscid fluid,

$$\frac{\partial^2}{\partial^2 t}\nabla^2 P + 4\frac{\partial^2}{\partial^2 z}P = 0. \tag{3}$$

This equation is usually referred to as the Poincaré equation. The corresponding boundary condition at the spherical bounding surfaces is

$$\left(s\frac{\partial}{\partial s}+z\frac{\partial}{\partial z}\right)\frac{\partial^2 P}{\partial t^2}+4z\frac{\partial P}{\partial z}+2\frac{\partial^2 P}{\partial t\,\partial\phi}=0. \tag{4}$$

The Poincaré equation, the simplest equation for three-dimensional wave motions in rotating fluids, is of primary importance in the understanding of many wave phenomena in geophysics and planetary physics. The equation is also of considerable interest from a mathematical standpoint as (3) and (4) have unusual mathematical properties (see §2).

The conventional β-plane solutions describing equatorially trapped gravity waves in a density-stratified fluid were found on the basis of the following assumptions (Matsuno 1966; Blandford 1966; see also the comprehensive monograph by Gill 1982): (*a*) shallow-water approximation, (*b*) neglecting radial acceleration in the equation of motion (the hydrostatic approximation), and (*c*) equatorial β-plane approximation. For comparison with the results of the present paper, we briefly describe the equatorially trapped gravity waves, which are related to the following partial differential equation (see Gill 1982 for details):

$$\frac{\partial}{\partial t}\left[\frac{1}{c^2}\left(\frac{\partial^2 v}{\partial t^2}+f^2 v\right)-\left(\frac{\partial^2 v}{\partial x^2}+\frac{\partial^2 v}{\partial y^2}\right)\right]-\beta\frac{\partial v}{\partial x}=0,$$

where $v=-u_\theta$, distance northward from the equator is denoted by $y=r(\frac{1}{2}\pi-\theta)$ and the eastward distance is $x=\phi r$, $c=(gH)^{\frac{1}{2}}$ is the speed of gravity wave with a constant depth H, and f and β are associated with the equatorial β-plane approximation

$$f=2\Omega\sin(\tfrac{1}{2}\pi-\theta)=(2\Omega/r)[r(\tfrac{1}{2}\pi-\theta)]=\beta y.$$

If we look for wave solutions proportional to $\exp \mathrm{i}(mx-\omega t)$, the above partial differential equation reduces to an ordinary differential equation

$$\frac{\mathrm{d}^2 v}{\mathrm{d}y^2}+\left(\frac{\omega^2}{c^2}-m^2-\frac{\beta m}{\omega}-\frac{\beta^2 y^2}{c^2}\right)v=0,$$

which has analytical solutions that vanish at infinitely large $\pm y$,

$$v=2^{-n/2}H_n[y(\beta/c)^{\frac{1}{2}}]\exp(-\beta y^2/2c)\cos(mx-\omega t),$$

H_n being a Hermite polynomial of order n. It is evident that the wave is an equatorially trapped wave, with amplitude decreasing exponentially from the equator $y=0$ and latitudinal radius dependent of the speed of the gravity wave c but independent of the azimuthal wavenumber m.

Most of the research conducted before 1970s on the three-dimensional problem in a rotating fluid sphere or spherical shell is summarized in Greenspan (1969). While the laboratory experiments of Aldridge & Toomre (1969) demonstrated the existence of axisymmetric spherical inertial oscillations, Stewartson & Rickard (1970) raised

series questions about the existence of continuous solutions of global scale ($m = 1$) in a thin-shell limit, where internal discontinuous layers on the characteristic surfaces of (3) become possible. Those internal discontinuous layers were observed experimentally in cylindrical geometry (see Greenspan 1969). The mathematical uncertainties lead Aldridge (1972) to the use of a variational principle for solutions of the axisymmetric oscillations in a thick spherical shell. Very little attention has been paid to the inertial waves that depart strongly from an axisymmetric symmetry (that is, $m \gg 1$). It is found, however, that strongly non-axisymmetric ($m \gg 1$) inertial waves with a simple-z structure can be most easily excited and sustained in an unstably stratified, nearly inviscid (small Prandtl number) fluid (Zhang & Busse 1987; Zhang 1992*b*). The exact three-dimensional solutions in the form of equatorially trapped boundary waves discussed in the present paper thus provide an essential framework not only for understanding but also attacking analytically the problem of spherical rotating (small Prandtl number) convection. Furthermore, although the general implicit forms of solutions for the Poincaré equation (either in modified oblate spheroidal coordinates or in cylindrical coordinates in which some roots of the associated Legendre function are involved in the summation of polynomials) have been available for a long time, it should be pointed out that very little can be learnt from the solutions of the general implicit forms and that systematic studies on the structure of the inertial waves have not been conducted.

The principal purpose of this paper is to examine subclasses of solutions of (3) and (4) in the form of equatorially trapped boundary waves. They are discovered under the following conditions: the scale of the wave motions is sufficiently small and the motion structure along the axis of rotation is sufficiently simple. A direct consequence is that the existence of an inner sphere and the condition of higher latitudes hardly affect the wave motions of this kind. We discuss some general properties of the Poincaré equation including classification of solutions according to their equatorial and rotational symmetries in §2. Solutions and properties of equatorially symmetric inertial waves are then examined in §3. This is followed by a discussion of equatorially antisymmetric inertial waves in §4. A supplementary numerical analysis for spherical shells with finite internal viscosity is presented in section §5.

2. Some properties of the Poincaré equation

Independence of the coefficients of (3) of the azimuthal variable ϕ and the time t allows us to seek azimuthally travelling wave solutions:

$$P = P(z, s)\, \mathrm{e}^{\mathrm{i}(m\phi+\omega t)},$$

where ω is the frequency of a wave. Equations (3) and (4) then become

$$\frac{1}{s}\frac{\partial}{\partial s}s\frac{\partial P}{\partial s}-\frac{m^2P}{s^2}+\left(1-\frac{4}{\omega^2}\right)\frac{\partial^2 P}{\partial z^2}=0, \tag{5}$$

$$s\frac{\partial P}{\partial s}+\frac{2m}{\omega}P+\left(1-\frac{4}{\omega^2}\right)z\frac{\partial P}{\partial z}=0. \tag{6}$$

It is of importance to note that the partial differential equation (5) is hyperbolic for $\omega < 2$ but boundary condition (6) is of the generalized Dirichlet kind: the problem of inertial waves is improperly posed in the Hadamard sense (Stewartson & Rickard 1970). Thus it is uncertain, particularly when an inner sphere is present, whether

continuous and physically acceptable solutions that satisfy the boundary condition (6) exist. Under the assumption that the solutions are well-behaved, however, many properties of the Poincaré equation are found and discussed by Greenspan (1964, 1969) (see also Lyttleton 1953). Separable solutions are possible in modified oblate spheroidal coordinates,

$$s^2 = \left(\frac{4}{4-\omega^2} - X^2\right)(1-Y^2), \tag{7}$$

$$z^2 = \left(\frac{4}{\omega^2} - 1\right)X^2Y^2. \tag{8}$$

The solutions can then be written

$$P(z,s) = P_l^m\left(X\left(1-\frac{\omega^2}{4}\right)^{\frac{1}{2}}\right)P_l^m(Y), \tag{9}$$

where P_l^m is an associated Legendre function. Substituting solution (9) into (6) yields an equation for the eigenfrequency ω:

$$mP_l^m(\alpha_k) - (1-\alpha_k^2)\frac{\mathrm{d}}{\mathrm{d}\alpha_k}P_l^m(\alpha_k) = 0, \tag{10}$$

where $\omega = 2\alpha_k$, and $k = 1, 2, 3, \ldots, K$, providing the third degree of freedom of the eigenfrequency, and the value of K is determined by the combination of l and m. It is also shown by Greenspan (1969) that ω is real and bounded by $-2 \leqslant \omega \leqslant 2$.

Faced with this complex three-dimensional eigenvalue problem, further classifications are necessary for gaining systematic understanding of the problem. One useful way is to divide solutions of the Poincaré equation into four subclasses according to their rotational and equatorial reflectional symmetry:

(*a*) $$(u_s, u_z, u_\phi)(s, z, \phi) = (u_s, -u_z, u_\phi)(s, -z, \phi + \Phi_0),$$

(*b*) $$(u_s, u_z, u_\phi)(s, z, \phi) = (-u_s, u_z, -u_\phi)(s, -z, \phi + \Phi_0),$$

(*c*) $$(u_s, u_z, u_\phi)(s, z, \phi) = (u_s, -u_z, u_\phi)(s, -z, \phi + 2\pi/m),$$

(*d*) $$(u_s, u_z, u_\phi)(s, z, \phi) = (-u_s, u_z, -u_\phi)(s, -z, \phi + 2\pi/m),$$

where Φ_0 is an arbitrary number. These symmetry properties can also be expressed in terms of a combination of l and m in (9): $m = 0$ and $l =$ even correspond to symmetry (*a*); $m = 0$ and $l =$ odd are for symmetry (*b*); $l-m =$ even and $m \geqslant 1$ represent symmetry (*c*); and $l-m =$ odd and $m \geqslant 1$ give rise to symmetry (*d*). Moreover, the combination of the indices (l, m, k) is also roughly indicative of the three-dimensional structure of the wave motions. While the wavenumber m indicates the azimuthal scale of the motions, the size of $l-m$ usually represents the degree of complexity in the z-direction. The larger value of $l-m$ usually corresponds to the more complicated z-structure. For a particular combination of $l-m$, it is the value of α (the third dimension k) that determines the radial structure.

Under certain physical conditions, only a small number of inertial modes can be excited. It is neither feasible nor necessary to investigate the whole spectrum of the problem; some physical mechanism should be adopted to discriminate among different subclasses of solutions. For rapidly rotating fluid systems, a very useful mechanism seems associated with the Taylor–Proudman theorem,

$$\partial \boldsymbol{u}/\partial z = 0,$$

which is a special case of (1). Fluid motions in many rotating fluid systems attempt to satisfy the Taylor–Proudman constraint: minimizing variations of the motions in the direction of the axis of rotation. An example of this are columnar convection rolls in rapidly rotating convective systems (Busse 1970; Busse & Or 1986; Zhang 1992*a*). As will be shown in a subsequent paper, it is only subclass (*c*) with the simplest z-structure ($l-m=2$) that can be excited and maintained by thermal convection. From the point of view of geophysical applications, the key subclasses of interest are likely to be related to the wave motions that have simple z-structure, i.e. the smallest values of $l-m$. We therefore concentrate attention on three subclasses of solutions of (5) and (6) that have the smallest values of $l-m$, forming three planes in three-dimensional eigenvalue space $(l-m, m, k)$, namely

symmetry (*d*): $\quad l-m=1, \quad m=1,2,\ldots\infty; \quad k=1,2\ldots K;$

symmetry (*c*): $\quad l-m=2, \quad m=1,2,\ldots\infty; \quad k=1,2\ldots K;$

symmetry (*d*): $\quad l-m=3, \quad m=1,2,\ldots\infty; \quad k=1,2\ldots K.$

Other subclasses with a more complicated z-structure ($l-m\geqslant 4$) are likely to be less important in most geophysical applications and will not be considered in this paper.

3. Equatorially symmetric waves

Equatorially symmetric wave motions (symmetry *c*) with the simplest z-structure are described by $l=m+2$. Equation (10) then gives rise to a quadratic equation which can be solved readily. Only two equatorially symmetric waves exist for this subclass: one propagates westward (ω^+) and other propagates eastward (ω^-):

$$\omega^+ = \frac{2}{l}\left(1+\left[\frac{l^2-1}{2l-1}\right]^{\frac{1}{2}}\right), \tag{11}$$

$$\omega^- = \frac{2}{l}\left(1-\left[\frac{l^2-1}{2l-1}\right]^{\frac{1}{2}}\right). \tag{12}$$

The corresponding solutions of (1) and (2) may be represented by

$$u_s = [A_s s^{l-1}+Bz^2 s^{l-3}+Cs^{l-3}]\sin(m\phi+\omega t), \tag{13}$$

$$u_\phi = [A_\phi s^{l-1}+Bz^2 s^{l-3}+Cs^{l-3}]\cos(m\phi+\omega t), \tag{14}$$

$$u_z = \frac{(2l-1)}{2} z s^{l-2}\sin(m\phi+\omega t), \tag{15}$$

where

$$A_\phi = \frac{(2l-1)(2l+l\omega-2\omega)}{8(1-l)}, \quad A_s = \frac{(2l-1)(2l+l\omega-4)}{8(1-l)},$$

$$B = \frac{(2l-1)(l-2)\omega^2}{4(\omega-2)}, \quad C = \frac{(l-2)}{(2-\omega)},$$

and they are normalized in such a way that

$$u_\phi(s=1,\phi=0,z=0,l=\infty) = -1.0.$$

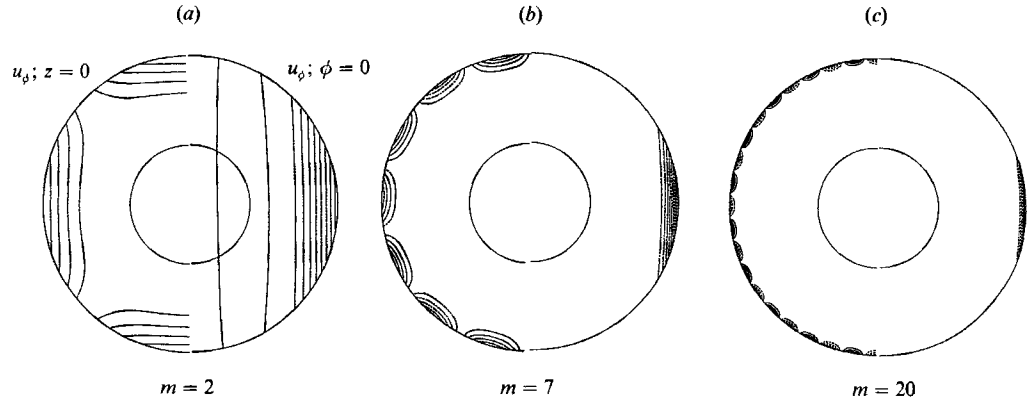

FIGURE 1. Contours of u_ϕ at the equatorial plane (on the left-hand side), and in a meridional plane (on the right-hand side) for the ω^- waves: (*a*) $m = 2$, (*b*) $m = 7$, and (*c*) $m = 20$.

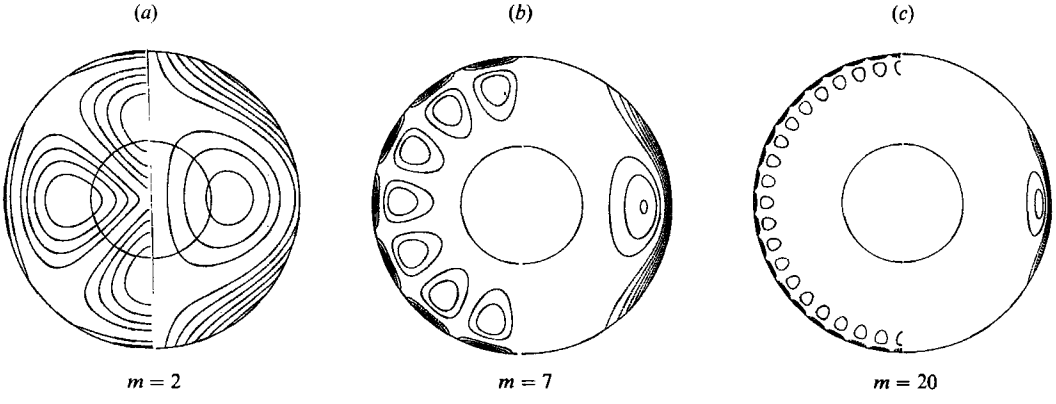

FIGURE 2. As in figure 1 but for the ω^+ waves.

The major reason why the solution is expressed in terms of velocity components is that the reduced pressure P is a much less convenient variable when higher-order terms like finite viscosity are involved (see §5).

This seemingly simple solution demonstrates one of the most extraordinary yet subtle forms of wave motion in rotating systems. Taking advantage of the properties of an azimuthally travelling wave, the profile of the wave structure can be illustrated in a frame of reference moving with the phase speed of a wave $c = -\omega/m$. Typical structure for the ω^- wave is shown in figure 1 for three different wavenumbers, and displayed in figure 2 is for the corresponding ω^+ wave. More detailed features of the solution can be seen in figure 3, where the velocity is shown as a function of θ and s for several typical wavenumbers. The most remarkable feature of the wave motions is their position: both the waves are trapped in an equatorial boundary region. In recent studies of spherical convection (Zhang 1992*a*), the crucial importance of spherical geometry on the pattern of convection is particularly emphasized. It appears that spherical geometry is essential to the form of inertial oscillations. In a rapidly rotating spherical system, the equatorial region characterized by strong curvature with respect to the axis of rotation forms an equatorial waveguide tube in which most of the wave energy is trapped. The concentration of the wave on the equatorial region is so high that the existence of an inner sphere and the whole area of middle and high latitudes are ignored when the scale of the wave motions are

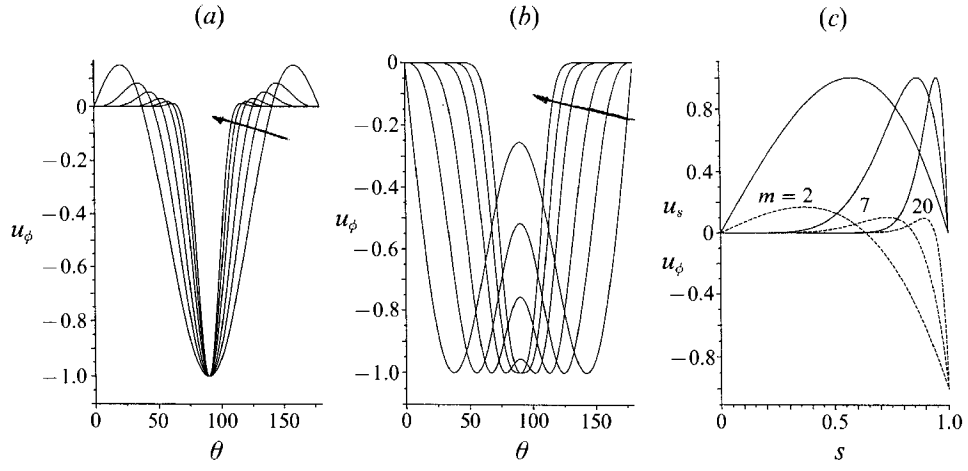

FIGURE 3. Normalized azimuthal velocity u_ϕ at the outer spherical surface as a function of θ: (*a*) ω^- waves and (*b*) ω^+ waves, where the azimuthal wavenumbers are (following the arrow) $m = 2$, 4, 7, 20, 30. (*c*) Radial dependences of u_ϕ (dashed lines) and u_s (solid lines) for $m = 2$, 7, 20 at the equatorial plane.

sufficiently small. By contrast, the equatorial waveguide tube cannot be provided by cylindrical geometry, and this may help to explain the existence of experimentally observed internal discontinuous layers on the characteristic surfaces (Greenspan 1969).

The properties of the equatorial waveguide tube are not obvious from the exact solutions but can be demonstrated more clearly in the large-wavenumber limit. Only the profile of the azimuthal component of the velocity, $u_\phi(r, \theta)$, is considered in detail, and other components can readily be studied in a similar way. We first examine the radial dependence for any fixed values of θ_0. We introduce a small parameter, $\delta = 1/m$, proportional to the wavelength of a wave, and a stretched boundary-layer coordinate,

$$x = \delta^{-1}(1-r).$$

We also expand the frequency of the waves in terms of $1/l$:

$$\omega = \omega_0 + \omega_1 + O(\delta^{\frac{3}{2}}) = \pm(2/l)^{\frac{1}{2}} + (2/l) + O(\delta^{\frac{3}{2}}).$$

Differentiating (14) with respect to r, we obtain

$$\frac{\partial u_\phi}{\partial r} = \frac{m}{r}[(1+\delta)A_\phi s^{l-1} + (1+\delta)Bs^{l-3}z^2 + (1-\delta)Cs^{l-3}].$$

To a first approximation, for sufficiently large wavenumbers, $\delta \ll 1$, the following equation can be derived:

$$\frac{\partial u_\phi}{\partial x} = -\frac{u_\phi}{1-\delta x}, \tag{16}$$

and the leading order gives

$$u_\phi(r) = u_\phi(1)\,\mathrm{e}^{-m(1-r)}. \tag{17}$$

It follows that the amplitude of u_ϕ decreases exponentially from the outer spherical surface, and that the characteristic thickness of the radial boundary is $O(1/m)$.

The amplitude not only decreases exponentially from the outer boundary in the radial direction but also from the equator towards higher latitudes. A similar

procedure can be applied to examining the latitudinal dependence at the outer spherical surface. There exist three peaks of u_ϕ as a function of θ, namely

$$\theta_1 = \tfrac{1}{2}\pi, \qquad \cos^2\theta_{2,3} = \frac{2B - A_\phi(l-1) - C(l-3)}{(B-A_\phi)(l-1)}.$$

While the u_ϕ for the ω^- wave reaches its maximum at the equator ($\theta_1 = \frac{1}{2}\pi$), the amplitude for the ω^+ wave displays two maxima (θ_2, θ_3) at finite latitudes for moderate wavenumbers, as evidenced by figure 3(*a*, *b*). However, the two maxima shift from finite latitudes towards the equator with increasing m, and disappear at $m = 20$ (see also figure 3*b*):

$$\cos^2\theta_{2,3}(l \leqslant 21) > 0; \quad \cos^2\theta_{2,3}(l \geqslant 22) < 0.$$

Consequently, both waves reach a maximum at the equator if the wavenumber $m \geqslant 20$. Differentiating (14) with respect to θ results in

$$\partial u_\phi/\partial\theta = \cot\theta[mu_\phi + g(\theta)],$$

where

$$g(\theta) = A_\phi \sin^{m+1}\theta - B(\sin^{m-1}\theta + \sin^{m+1}\theta) - C\sin^{m-1}\theta.$$

The leading order gives rise to

$$u_\phi(\theta) = [(A_\phi + C) + \delta(A_\phi - 2B - C)]\,\mathrm{e}^{-m(\pi/2-\theta)^2/2} - \delta(A_\phi - 2B - C),$$

which yields

$$u_\phi(\theta) = (u_\phi(\tfrac{1}{2}\pi) + 2\omega_0)\,\mathrm{e}^{-m(\pi/2-\theta)^2/2} - 2\omega_0 + O(\delta). \tag{18}$$

It is evident that the characteristic latitude to which the wave motions extend from the equator is $L_1 = (2/m)^{\frac{1}{2}}$.

The zone in the vicinity of the equator therefore forms an equatorial-waveguide tube of radial scale $1/m$ and latitudinal scale $(2/m)^{\frac{1}{2}}$; we refer this type of three-dimensional wave as equatorially trapped boundary waves. It immediately becomes obvious that the geometrical factor of an inner core exerts a weak influence on wave motions of this type if the wavenumber of a wave satisfies

$$m > \frac{\pi(1+\eta)}{2(1-\eta)}, \tag{19}$$

where $\eta = r_i/r_o$, the radius ratio of a shell. The finding of equatorially trapped boundary waves provides a simple answer to the mathematical difficulties of the Poincaré equation in a rotating spherical fluid shell: the effects of an inner sphere on this subclass may be safely ignored if condition (19) is well satisfied.

4. Equatorially antisymmetric waves

Equatorially antisymmetric waves (symmetry (*d*), $l - m < 4$) similarly show equatorial trapping, and the corresponding equatorial waveguide tube is characterized by similar scales. The simplest subclass of equatorially antisymmetric waves is represented by $l - m = 1$, and (10) then gives the eigenfrequency

$$\omega = 2/l.$$

The structure of the wave motions, in contrast to the case of $l - m > 1$ is independent of the frequency ω. In addition, the fluid motions are nearly two-dimensional,

$\partial u_z/\partial z = 0$, and a stream function, Ψ, in a plane parallel to the equatorial plane can therefore be introduced. The solutions of (5) and (6) for $l-m = 1$ may be expressed by

$$u_z = -s^{l-1} \sin(m\phi + \omega t), \tag{20}$$

$$\Psi = \frac{1}{l-1} s^{l-1} z \cos(m\phi + \omega t), \tag{21}$$

where

$$u_s = -\frac{1}{s}\frac{\partial \Psi}{\partial \phi}; \quad u_\phi = \frac{\partial \Psi}{\partial s}.$$

It is also interesting to note that the wave motions in this case are purely toroidal and two-dimensional in spherical coordinates: $u_r = u_z z + u_s s \equiv 0$. The peaks of the amplitude of the azimuthal component at the outer spherical surface are located at

$$\theta_c = \tfrac{1}{2}\pi \pm \sin^{-1}(1/m)^{\frac{1}{2}},$$

which approaches to the equator with increasing values of the azimuthal wavenumber. In a similar way, we can derive the following equations:

$$\frac{\partial u_\phi}{\partial x} = -\frac{u_\phi}{1-\delta x}; \quad \frac{1}{u_\phi}\frac{\partial u_\phi}{\partial \theta} = -\frac{2(1-m\cos^2\theta)}{\sin(2\theta)}$$

and the leading order leads to

$$\frac{\partial u_\phi}{\partial x} = -u_\phi; \quad \frac{1}{u_\phi}\frac{\partial u_\phi}{\partial \theta} = -2m(\theta-\theta_c).$$

The radial and latitudinal dependences of u_ϕ again can be expressed as

$$u_\phi(r) = u(1)\, e^{-m(1-r)}; \quad u_\phi(\theta) = u(\theta_c)\, e^{-m(\theta-\theta_c)^2}. \tag{22}$$

The amplitude decreases exponentially both radially from the outer spherical surface and latitudinally from the equator with characteristic scales $L_r = (1/m)$ and $L_l = (1/m)^{\frac{1}{2}}$. This particular case was studied by Malkus (1968).

Equatorially antisymmetric waves with more complex spatial structure are described by $l-m = 3$, and the corresponding frequencies of the wave motions are related to the roots of the following cubic equation

$$F(\alpha) = -\tfrac{1}{3}(2l-1)\, l\alpha^3 + (2l-1)\,\alpha^2 + (l-2)\,\alpha - 1 = 0, \tag{23}$$

where α is $\frac{1}{2}\omega$. The general properties of the eigenfrequencies may be obtained without actually solving the cubic equation. First, the geostrophic mode ($\omega = 0$) cannot satisfy (5) and (6) with $l-m = 3$, since $F(0) = -1$. Secondly, there exist three real eigenvalues in the region $-2 < \omega < 2$, corresponding to three different waves if $m \geqslant 1$. This is because the criteria of the cubic equation (e.g. Abramowitz & Stegun 1972)

$$\Delta = -\frac{(l+1)^2(l-2)}{l^3(2l-1)^3},$$

is always negative, and

$$F(1) = -\tfrac{2}{3}(l-3)(l-2) < 0; \quad F(-1) = \tfrac{2}{3}l(l+1) > 0,$$

hold for every non-zero wavenumber. It is also straightforward to show that there are two solutions for $\partial F(\alpha)/\partial\alpha = 0$: $-1.0 < \alpha_1 < 0$ and $0 < \alpha_2 < 1.0$. Of the three

antisymmetric waves for any non-zero wavenumber, therefore, two must propagate westward ($\omega > 0$) and the other propagates eastward ($\omega < 0$). The precise values of the eigenfrequency can be expressed by the following formulae:

$$\omega_1 = \frac{4}{l}\left[\frac{(l^2-1)^{\frac{1}{2}}}{(2l-1)^{\frac{1}{2}}}\cos\left(\tfrac{1}{3}\gamma\right)+\tfrac{1}{2}\right], \tag{24}$$

$$\omega_2 = \frac{4}{l}\left[\frac{(l^2-1)^{\frac{1}{2}}}{(2l-1)^{\frac{1}{2}}}\cos\left(\tfrac{1}{3}\gamma+\tfrac{2}{3}\pi\right)+\tfrac{1}{2}\right], \tag{25}$$

$$\omega_3 = \frac{4}{l}\left[\frac{(l^2-1)^{\frac{1}{2}}}{(2l-1)^{\frac{1}{2}}}\cos\left(\tfrac{1}{3}\gamma+\tfrac{4}{3}\pi\right)+\tfrac{1}{2}\right], \tag{26}$$

where $$\gamma = \cos^{-1}(-1)\left[\frac{(2l-1)}{(l+1)(l-1)^3}\right]^{\frac{1}{2}}.$$

The corresponding solutions for (3) and (4) may be represented by

$$u_s = z[A_s s^{l-2} + Bz^2 s^{l-4} + Cs^{l-4}]\sin(m\phi+\omega t), \tag{27}$$

$$u_\phi = z[A_\phi s^{l-2} + Bz^2 s^{l-4} + Cs^{l-4}]\cos(m\phi+\omega t), \tag{28}$$

$$u_z = -\frac{1}{\omega}[A_z s^{l-1} + B_z z^2 s^{l-3} + s^{l-3}]\sin(m\phi+\omega t), \tag{29}$$

where

$$A_s = \frac{(2l-1)(2l+l\omega-\omega-6)}{8(2-l)}, \quad A_\phi = \frac{(2l-1)(2l+l\omega-3\omega-2)}{8(2-l)};$$

$$B = -\frac{(2l-1)(l-3)\omega^2}{12(2-\omega)}, \quad C = \frac{(l-3)}{(2-\omega)};$$

$$A_z = \frac{(2l-1)(4-\omega^2)}{8(2-l)}, \quad B_z = -\frac{(2l-1)\omega^2}{4}.$$

It is straightforward to show that the same expression (17) for the radial dependence can be obtained for the subclass of $l-m = 3$, provided that the wavenumber satisfies $m \gg 2$. The latitudinal dependence, however, is somewhat more complicated, and is described by

$$\cos 2\theta \frac{\partial u_\phi}{\partial \theta} = 2mu_\phi[(1+O(\delta))\cos^2\theta - \delta\sin^2\theta)] - 4B\sin^{m+1}\theta\cos^3\theta,$$

where the second term on the right-hand side is associated with the secondary effects of the θ-dependence (similar to the term $2\omega_0$ in (18)). If this term is neglected, we again readily show that the leading order leads to

$$u_\phi(\theta) = u(\theta_c)\,e^{-m(\theta-\theta_c)^2}$$

where $$\theta_c = \tfrac{1}{2}\pi \pm \tan^{-1}(1/m)^{\frac{1}{2}}.$$

In the first approximation, the amplitude of u_ϕ again decreases exponentially, radially from the outer spherical surface and latitudinally from the peak, regardless of the sign and size of the frequency. The dependence of u_ϕ on θ for different frequencies at the outer spherical surface is shown in figure 4 for $m = 3$ and 20.

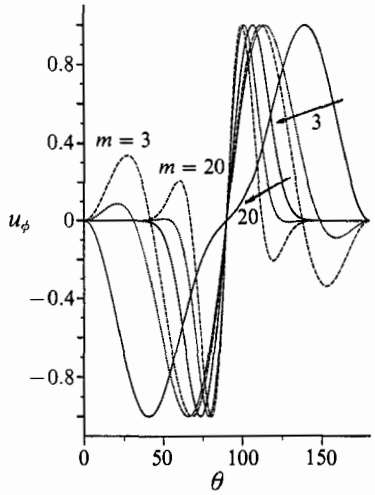

FIGURE 4. Normalized azimuthal velocity u_ϕ at the outer spherical surface as a function of θ for the azimuthal wavenumbers $m = 3$ and 20 ($l-m = 3$). The frequencies are (following the arrow) $\omega = 1.3402$, -0.7181, 0.3779 for $m = 3$ and $\omega = 0.6015$, -0.4303, 0.08959 for $m = 20$.

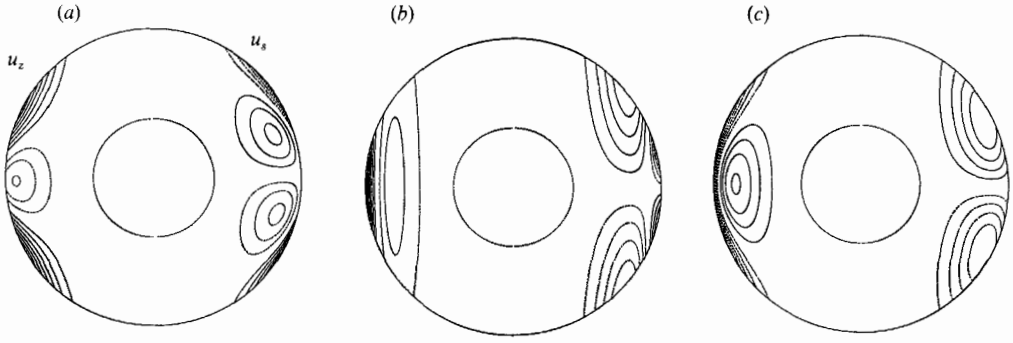

FIGURE 5. Contours of u_z (on the left-hand side) and u_s (on the right-hand side) in a meridional plane for (*a*) $\omega = 0.9832$, (*b*) $\omega = 0.2148$ and (*c*) $\omega = -0.5980$ with $m = 7$, $l-m = 3$.

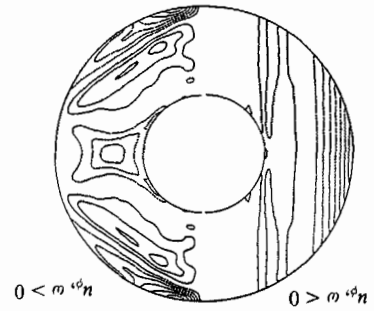

FIGURE 6. Contours of u_ϕ in a meridional plane from the Greenspan equation at $r_i/r_0 = 0.4$ and $m = 2$. The ω^- solution is on the left-hand side, and the ω^+ solution on the right-hand side.

Displayed in figure 5 are typical structures for three equatorially antisymmetric boundary waves at $m = 7$ with $\omega = 0.9832, 0.2148$ and -0.5980. Though the detailed structured of the solutions is quite different, the character of the equatorial trapping is essentially the same, particularly when the azimuthal wavenumber is large. It is

not surprising that u_z in figure 4 displays a profile similar to that of u_ϕ for the case $l-m=2$ in figures 1 and 2 because of the similar forms and same symmetries of (29) and (14).

5. The Greenspan equation in spherical shells

Ignoring the mathematical uncertainties of the problem, the solutions of (5) and (6) appear to be sound, and are unaffected by the presence of an inner sphere if the scale of the wave is sufficiently small. One way, however, to gain a better understanding of the problem, and particularly of the effects of an inner core on the large-scale waves, is to solve a mathematically well-defined but closely related problem in rotating spherical shells. An obvious choice is to take into account the effects of finite viscosity $\nu \neq 0$, described by the Greenspan equation (Greenspan 1969)

$$\left[\frac{\partial}{\partial t}-E\nabla^2\right]^2\nabla^2 P+4\frac{\partial^2 P}{\partial^2 z}=0, \tag{30}$$

where E is the Ekman number here defined as $E=\nu/\Omega(r_o-r_i)^2$, and the characteristic lengthscale is the thickness of a spherical shell. Stress-free boundary conditions are assumed owing largely to the numerical difficulties of treating rigid boundary conditions. A comparison between (5) in a sphere and (30) in spherical shells can be achieved in the limit of small Ekman numbers. A simple velocity boundary condition in terms of the pressure P like (6), however, cannot be obtained for the stress-free boundary. We therefore expand the velocity $\boldsymbol{u}$ as a sum of poloidal and toroidal vectors

$$\boldsymbol{u}=\nabla\times\nabla\times\boldsymbol{r}v+\nabla\times\boldsymbol{r}w.$$

Making use of this expression, two independent governing scalar equations, equivalent to (30), can be derived (see, for example, Zhang 1992*a*),

$$\left[\left(E\nabla^2-\frac{\partial}{\partial t}\right)\mathscr{L}+2\frac{\partial}{\partial\phi}\right]\nabla^2 v+2\mathscr{Q}w=0, \tag{31}$$

$$\left[\left(E\nabla^2-\frac{\partial}{\partial t}\right)\mathscr{L}+2\frac{\partial}{\partial\phi}\right]w-2\mathscr{Q}v=0. \tag{32}$$

The differential operators, $\mathscr{L}$ and $\mathscr{Q}$, are defined as

$$\mathscr{L}=-r^2\nabla^2+\frac{\partial}{\partial r}r^2\frac{\partial}{\partial r},$$

$$\mathscr{Q}=r\cos\theta\nabla^2-\left(\mathscr{L}+r\frac{\partial}{\partial r}\right)\left(\cos\theta\frac{\partial}{\partial r}-\frac{\sin\theta}{r}\frac{\partial}{\partial\theta}\right).$$

Equations (31) and (32) are solved subject to the following conditions at the inner and outer bounding spherical surfaces:

$$v=\frac{\partial^2 v}{\partial r^2}=\frac{\partial}{\partial r}\left(\frac{w}{r}\right)=0. \tag{33}$$

The method for solving the above equations is the Galerkin spectral method, similar to that described by Zhang (1992*a*).

In contrast to the inviscid case, the problem defined by (31)–(33) is a well-defined

m, l	$\eta = 0, E = 0$	$\eta = 0.2$	$\eta = 0.4, E = 10^{-4}$	$\eta = 0.6, E = 10^{-4}$
2, 4	$-$i0.2319	$-0.2313\epsilon - $i0.2305, $E = 10^{-4}$	$-0.3208\epsilon - $i0.2124	$-0.2868\epsilon - $i0.1631
2, 4	$+$i1.2319	$-0.3369\epsilon + $i1.2316, $E = 10^{-4}$	$-0.6826\epsilon + $i1.6153	$-0.3464\epsilon + $i1.5579
7, 9	$-$i0.2598	$-0.1190\epsilon - $i0.2597, $E = 10^{-5}$	$-0.6685\epsilon - $i0.2595	$-0.4253\epsilon - $i0.2567
7, 9	$+$i0.7043	$-0.1237\epsilon + $i0.7042, $E = 10^{-5}$	$-0.6909\epsilon + $i0.7041	$-0.5253\epsilon + $i0.6986
2, 3	$+$i0.6667	$-0.0444\epsilon + $i0.6667, $E = 10^{-4}$	$-0.0248\epsilon + $i0.6667	$-0.0106\epsilon + $i0.6667
7, 8	$+$i0.2500	$-0.0666\epsilon + $i0.2500, $E = 10^{-5}$	$-0.3409\epsilon + $i0.2498	$-0.1564\epsilon + $i0.2499
7, 10	$-$i0.5980	$-0.1767\epsilon - $i0.5978, $E = 10^{-5}$	$-0.9935\epsilon - $i0.5976	$-0.5591\epsilon - $i0.5979
7, 10	$+$i0.2148	$-0.2703\epsilon + $i0.2149, $E = 10^{-5}$	$-1.0026\epsilon + $i0.2126	$-0.5144\epsilon + $i0.2138
7, 10	$+$i0.9832	$-0.1872\epsilon + $i0.9830, $E = 10^{-5}$	$-1.0357\epsilon + $i0.9828	$-0.6909\epsilon + $i0.9828

TABLE 1. Eigenvalues at different values of η and E, where $\epsilon = 10^{-2}$

linear decay problem, where the decay rate, σ, is dependent on the values of E and m, and is of the order of $\sigma = O(m^2E)$ in the case of stress-free boundary conditions. In the limit of small E, the form and frequency of the decay mode in a spherical shell should approach those given by the solutions of the inertial wave in an inviscid full sphere if there are no internal discontinuities, if the waves are trapped in the equatorial waveguide tube and if the azimuthal wavenumber is sufficiently large. The numerical analysis then serves to confirm the impression of the properties of the equatorially trapped boundary waves gained from analytical solutions in a full sphere.

For a given value of the azimuthal wavenumber, it is found that the modes with the simplest z-structure (corresponding to (9) with the smallest values of $l-m$) always have the smallest decay rate. This behaviour is expected because of the decreasing viscous dissipation with simpler z-structure. Table 1 shows some typical examples of the results of (31)–(33) for different wavenumbers and symmetries. The analytical results of (5) (the case $\eta = 0$, $E = 0$) are also included for comparison. When (19) is well satisfied, all eigenfrequencies for an inviscid full sphere are recovered in spherical shells and, furthermore, the structure of the corresponding eigenvectors is nearly identical to that of a full sphere. The slight differences between a sphere and spherical shells in table 1 arise from the fact that the wave must satisfy the stress-free boundaries in addition to $u_r = 0$, occurring mainly at the outer spherical surface. When the condition (19) is not or only roughly satisfied (that is, the typical radial scale of the wave is larger than the thickness of the shell, for instance, $m = 2$ at $\eta = 0.4$), the modifications in the wave structure and frequency are more noticeable, and could be substantial because the changes in both the inner and outer boundaries are necessary in order to satisfy the boundary conditions. Figure 6, which can be compared to figures 1 (*a*) and 2 (*a*), illustrates how these changes are made. The effects of the inner core are much less important for the ω^- wave that has a nearly z-independent profile; in the case of the ω^+ wave, however, the big cell passing through the inner core in figure 2 (*a*) is split into small cells to satisfy the boundary conditions.

6. Concluding remarks

The finding of the equatorially trapped boundary waves reported in this paper could be of great benefit to the understanding of many geophysical fluid phenomena ranging from hydrodynamic waves to magnetohydrodynamic oscillations. With a particular choice of a basic magnetic field, the problem of magnetohydrodynamic

oscillations is described by exactly the same equations (5) and (6) except that the frequency is a function of the strength of the imposed magnetic field (Malkus 1967; Hide & Stewartson 1972), though the particular choice of the basic magnetic field phases out some important and physically interesting magnetic instabilities. On the basis of the analytical solutions discussed in this paper, analytical solutions of convection in rotating spherical systems can, for the first time, be obtained for small-Prandtl-number fluids (Zhang 1992*b*). In addition, the phenomenon of the equatorial trapped wave has been found and discussed extensively in the context of ocean and atmosphere tropic dynamics (e.g. Gill 1982). It is of importance, however, to note that while the conventional β-plane solutions discussed in §1 and those derived in §§3 and 4 both exhibit equatorial trapping, in reality they are solutions to different physical problems as clearly indicated by the dependence of their latitudinal scales.

Recent identifications of inertial waves in the Earth's fluid core from superconducting gravimetric data (Aldridge & Lumb 1987) created much new interest in this classical problem. There appears growing recognition by the geophysical community that inertial-wave observation may provide important direct information about the physical and dynamical properties of the Earth's interior (Aldridge & Lumb 1987; Smylie 1988; Crossley, Hinderer & Legros 1991). But on almost every major question, the difficulties encountered can be traced back to the fundamental mathematical uncertainties of the Poincaré equation. One of them is the effect of an inner sphere on the solutions obtained from a full sphere, which is of primary importance with regard to geophysical applications because of the presence of the inner solid core of the Earth. The results of this paper indicate that the effect of an inner sphere is likely to be small with azimuthal wavenumber $m > 3$.

There was scant evidence of the existence of discontinuities across the characteristic surface for the cases studied in this paper. However, it is not clear whether the singularities found by Stewartson & Rickard (1970) by studying the perturbations of the solutions of Longuet-Higgins (1964) can be attributed to the fact that the limits of small wavenumber ($m = 1$) and thin shell is assumed in their analysis. It appears that the singularities discussed by Stewartson & Rickard (1970) are at least insignificant in the solutions of the inertial wave that attempt to satisfy the Taylor–Proudman condition (the simple z-structure), and are trapped in the equatorial waveguide tube in a thick rotating spherical shell like the fluid core of the Earth.

This work is supported by the SERC and, while I was at Leeds University, partially supported by the Leverhulme Trust.

REFERENCES

Abramowitz, M. & Stegun, I. S. 1972 *Handbook of Mathematical Functions*. Dover.

Aldridge, K. D. 1972 Axisymmetric oscillations of a fluid in a rotating spherical shell. *Mathematika* **19**, 163–168.

Aldridge, K. D. & Lumb, L. I. 1987 Inertial waves identified in the Earth's fluid outer core. *Nature* **325**, 421–423.

Aldridge, K. D. & Toomre, A. 1989 Axisymmetric inertial oscillations of a fluid in a rotating spherical container. *J. Fluid Mech.* **37**, 307–323.

Blandford, R. R. 1966 Mixed gravity–Rossby waves in the ocean. *Deep-Sea Res.* **13**, 941–961.

Bryan, G. H. 1889 The waves on a rotating liquid spheroid of finite ellipticity. *Phil. Trans. R. Soc. Lond.* A **180**, 187–219.

Busse, F. H. 1970 Thermal instabilities in rapidly rotating systems. *J. Fluid Mech.* **44**, 441–460.

BUSSE, F. H. 1982 Thermal convection in rotating systems. In *Proc. 9th US Natl Cong. Appl. Mech.*, pp. 299–305. ASME.

BUSSE, F. H. & OR, A. C. 1986 Convection in a rotating cylindrical annulus: thermal Rossby waves. *J. Fluid Mech.* **166**, 173–187.

CROSSLEY, D. J., HINDERER, J. & LEGROS, H. 1991 On the excitation, detection and damping of core modes. *Phys. Earth Planet. Inter.* **68**, 97–116.

GILL, A. E. 1982 *Atmosphere–Ocean Dynamics*. Academic.

GREENSPAN, H. P. 1964 On the transient motion of a contained rotating fluid motions. *J. Fluid Mech.* **21**, 673–679.

GREENSPAN, H. P. 1969 *The Theory of Rotating fluids*. Cambridge University Press.

HIDE, R. & STEWARTSON, K. 1972 Hydrodynamics oscillations of the Earth's core. *Rev. Geophys. Space Phys.* **10**, 579–598.

LONGUET-HIGGINS, M. S. 1964 Planetary waves on a rotating sphere. *Phil. Trans. R. Soc. Lond.* A **279**, 446–473.

LYTTLETON, R. A. 1953 *The Stability of Rotating Liquid Masses*. Cambridge University Press.

MALKUS, W. V. R. 1967 Hydromagnetic planetary waves. *J. Fluid Mech.* **28**, 793–802.

MALKUS, W. V. R. 1968 Equatorial planetary waves. *Tellus* **20**, 545–547.

MATSUNO, T. 1966 Quasi-geostrophic motions in the equatorial area. *J. Met. Soc. Japan* **44**, 25–43.

SMYLIE, D. E. 1988 Variational calculation of core modes in realistic Earth models. In *Structure and Dynamics of Earth's Deep Interior* (ed. D. E. Smylie & R. Hide), pp. 23–28.

STEWARTSON, K. & RICKARD, J. R. A. 1970 Pathological oscillation of a rotating fluid. *J. Fluid Mech.* **35**, 759–773.

ZHANG, K. 1992*a* Spiralling columnar convection in rapidly rotating spherical fluid shells. *J. Fluid Mech.* **236**, 535–556.

ZHANG, K. 1992*b* On the coupling between the Poincaré equation and convection *J. Fluid Mech.* (submitted).

ZHANG, K. & BUSSE, F. 1987 On the onset of convection in rotating spherical shells. *Geophys. Astrophys. Fluid Dyn.* **39**, 119–147.